Proceedings of the Canadian Society for Mechanical Engineering International Congress 2021
CSME Congress 2021
June 27-30, 2021, Charlottetown, PE, Canada

SIMULTANEOUS TOPOLOGY AND COMPOSITE LAY-UP OPTIMIZATION

Rubens Bohrer[1], Il Yong Kim[1*]
[1]Department of Mechanical and Materials Engineering, Queen's University, Kingston, Ontario, Canada
*iykim@me.queensu.ca

Abstract—With the advances in manufacturing and design methods, engineers have been constantly pushed to improve mechanical components performance by minimizing part weight, maximize stiffness and optimize material usage. Tools such as topology optimization has been widely used to support the development of new components. While the optimization process for metallic components is well stablished, composite materials optimization still possess challenges to designers, especially due to the plies stacking sequence definition. The recent advances in 3D printed composite additive manufacturing have brought a new alternative to the composite manufacturing adding geometric freedom and challenges on the definition of the optimum material layout and lay-up. Thus, this paper expands upon existing mathematical methods by providing an algorithm to simultaneously minimizing the material distribution and the laminate stacking sequence of composite plates. Lamination parameters are used as design variables to optimize the laminate stacking sequence avoiding local optimum solutions and reducing the number of designable variables. Once the optimum topology and set of lamination parameters are defined, angle retrieval is performed to define the optimum plies orientation. Two problem examples are solved to illustrate the applicability of this approach.

Keywords-component; Additive manufactuing; simultaneous, topology optimization; stacking sequence optimization

I. INTRODUCTION

Additive Manufacturing (AM) has been shifting from its roots on the production of simple plastic prototypes to printers that can handle materials ranging from plastic to titanium [1], and more recently short and continuous composite fibers. Whilst metal AM parts have already been applied in aircrafts as structural component [2-4], composite AM, especially continuous fiber, is still a relatively new and undeveloped research topic which possesses significant challenges [5].

Besides the fact that companies such as MarkForged [6] and Continuous Composites [7] have been advancing on the development of continuous fiber 3D printers, there is still the need for methods and tools able to generate paths that can allow for the fabrication of parts possessing enhanced mechanical properties [8].

Topology optimization (TO) has been reported by many authors as a method to generate unconventional load paths [9-12]. TO was used by [13], for instance, in the conceptual design of an automotive engine cradle showing significant mass reduction results. Reference [14] on the other hand, investigated TO on a pre-stiffened bulkhead with a frequency-based problem, where the first frequency eigenfrequency is maximized subjected to a mass ratio of the component.

In the last decade, there has been an increase interest in the development of TO applied to additive manufacturing techniques. The cost of 3D printed components, for example, has been investigated by [15] and [16]. In their work, TO was applied to additive manufacturing seeking to maximize the component's stiffness considering the time and supported material required for the design. Design for additive manufacturing has also been considered by [17] and [18] where the simultaneous TO and build orientation optimization were used to achieve optimum designs that minimizes the manufacturing cost.

Common to most of the TO applied to additive manufacturing techniques is the use of isotropic materials as candidate material. Nevertheless, with the increasing application of composite materials on the design of lightweight structures, especially due to their high strength to weight ratio, there is an increased need for methods and tools that allow designers to exploit the unidirectional composite properties along with the manufacturing freedom delivered by additive manufacturing processes.

This article proposes an algorithm to simultaneously perform TO and stacking sequence optimization of unidirectional composite plates. Two sets of design variables are simultaneously solved by the optimizer, the TO artificial densities and the stacking sequence design variables. Stacking sequence design variables are defined through a set of lamination parameters (LPs) that overcomes the lack of convexity of the objective function inherent of lamination angles as well as limits the maximum number of design variables independently of the number of angle plies.

Topology Optimization was introduced as a homogenization method to provide the optimal shape and topology of mechanical elements by [19]. Shortly after, [20] proposed the application of artificial densities as design variables as a method of removing the discrete nature of the

problem by the introduction of a density function that is a continuous design variable, the process was afterwards denominated as Solid Isotropic Material with Penalization (SIMP) by [21].

With regards to the stacking sequence optimization, many different optimization approaches have been proposed in the literature. For instance, early attempts were done by [22] that proposed to minimize the weight of symmetric fiber composite-laminates subjected to strength and stiffness constraints using the layer thickness as design variables at specific orientation angles. Results showed that depending on the load and boundary conditions the thickness of specific plies were reduced to zero indicating that the vanished ply was not contributing to the performance measure of the optimization problem. Reference [23], on the other hand, used ply angles as design variables. They minimized the Tsai-Wu failure criteria as with strength restrictions for composite laminates with few plies – no more than three design variables were used in the design optimization process.

In composite lay-up optimization, one of the major problems of using ply angles as design variables is the lack of convexity of the objective function and thus the existence of local optima [24]. Due to this fact, several approaches have been proposed in order to optimize composite stacking sequence in different applications, examples are [25] and [26] who used genetic algorithms and simulated annealing, respectively, to minimize the mass of composite plates subjected to transversal impact with plies angles as design variables.

In this context, parametrization of the ply orientation via the LPs presents an alternative to overcome the difficulties to the lack of convexity of the objective function. Figure I illustrates both LPs and fiber angles spaces in the optimization process, in this illustrative example, it is possible to notice that the fiber angles space (solid line) is represented by a non-convex function $f(\theta)$ with two local minima (points 2 and 4), while the LPs domain (dotted line) is represented by a convex function $f(\xi)$ which leads to a unique optimum point (dark point).

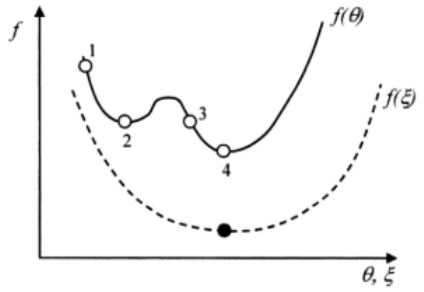

FIGURE I – ILLUSTRATION OF THE OPTIMIZATION PROCESS IN BOTH SPACES OF THE LAMINATION PARAMETERS AND THE FIBERS ORIENTATION [27].

Attempts to simultaneously optimize the shape and stacking sequence of composite laminates have been proposed. For example, gradient-based cellular automata optimization was proposed by [28] to solve the TO and fiber path design of composite layers. Reference [29] proposed a two-step minimization problem to solve the stackings sequence optimization using LPs and the TO problem sequentially. Reference [30] proposed a method for solving the compliant mechanism optimization considering fiber orientation and topology optimization.

II. OPTIMIZATION PROBLEM STATEMENT

A. Traditional TO Statement

The objective of TO problems is to define the materials distribution over a design domain such as the objective function is minimized subject to a constraint. The well-known compliance minimization subject to volume fraction problem statement is presented in (1).

$$\begin{aligned} \min \quad & \mathrm{C}(\boldsymbol{u},\boldsymbol{\rho}) = \boldsymbol{u}(\boldsymbol{\rho})^T \boldsymbol{k}(\rho)\boldsymbol{u}(\boldsymbol{\rho}) \\ s.t. \quad & \frac{V(\rho)}{V_i} \le \bar{V} \\ & \boldsymbol{Ku}=\boldsymbol{f} \text{ for static problems} \\ & \forall\rho,\ \rho^i \in (0,1],\ \ i=1,2,....,m \end{aligned} \tag{1}$$

where $\mathrm{C}(\boldsymbol{u},\boldsymbol{\rho})$ is the compliance that is a function of the displacement vector $\boldsymbol{u}$ and the artificial design variables $\boldsymbol{\rho}$, $\boldsymbol{k}$ is the element stiffness matrix, $V(\rho)$, V_i and $\bar{V}$ are the penalized element volume, the initial volume of the design space and the volume fraction constraint, respectively, $\boldsymbol{f}$ is the nodal forces vector and m is the number of elements in the design space.

B. Lamination parameters

Lamination parameters are defined as trigonometric functions of the ply orientations. In this article, only the extensional matrix is considered, thus the set of four extensional LPs can be defined as (2):

$$\xi^{A}_{\{1,2,3,4\}} = \frac{1}{T}\sum_{k=1}^{n}(h_k - h_{k+1})\{\cos 2\theta_k,\ sin2\theta_k,\ \cos 4\theta_k,\ sin4\theta_k\} \tag{2}$$

where θ_k is the ply orientation angle, T is the laminate thickness, n is the number of layers and h_k is the distance from the center of the laminate to the interface between the k^{th} and the k^{th+1} layer.

The composite extensional material stiffness matrix [A], can be defined using the extensional LPs as (3):

$$[A] = T\begin{bmatrix} U_E + \xi_1 U_{\Delta C} + \xi_3 U_{\upsilon C} & U_E - 2U_G - \xi_3 U_{\upsilon C} & \frac{\xi_2}{2}U_{\Delta C} + \xi_4 U_{\upsilon C} \\ sym & U_E - \xi_1 U_{\Delta C} + \xi_3 U_{\upsilon C} & \frac{\xi_2}{2}U_{\Delta C} - \xi_4 U_{\upsilon C} \\ sym & sym & U_G - \xi_3 U_{\upsilon C} \end{bmatrix} \tag{3}$$

where $\xi_i^A = \xi_i$, $i = 1,2,3,4$, and U_E , U_G , $U_{\Delta C}$ and $U_{\upsilon C}$ are the stiffness invariants defined in (4):

$$\begin{aligned} U_E &= \left(3Q_{11} + 3Q_{22} + 2Q_{12} + 4Q_{66}\right)/8 \\ U_G &= \left(Q_{11} + Q_{22} - 2Q_{12} + 4Q_{66}\right)/8 \\ U_{\Delta c} &= \left(Q_{11} - Q_{22}\right)/2 \\ U_{VC} &= \left(Q_{11} + Q_{22} - 2Q_{12} - 4Q_{66}\right)/8 \end{aligned} \tag{4}$$

where Q_{ij} are the reduced stiffness for unidirectional lamina defined as (5):

$$\begin{aligned} Q_{11} &= E_1/(1-\nu_{12}\nu_{21}) \qquad Q_{12} = \nu_{12}E_2/(1-\nu_{12}\nu_{21}) \\ Q_{22} &= E_2/(1-\nu_{12}\nu_{21}) \qquad Q_{66} = G_{12} \end{aligned} \tag{5}$$

where E_1 , E_2 , G_{12} are the longitudinal, transverse and shear moduli, respectively, and ν_{12} and ν_{21} are the Poisson's ratio.

C. Feasible Region

By definition, the LPs can assign values within the bounds of $-1.0 \le \xi_i \le 1.0$, $i = 1,2,3,4$. Nevertheless, LPs bounds are not sufficient to guarantee that a combination among the LPs represents a feasible lay-up. Thus, further constraints to define the feasible region of the set of LPs need to be defined.

The feasible region has been firstly described by [31], who defined the feasible region based on some lamination parameters relations. Specifically, the author determined the feasible region described by the relation between two in-plane stiffness as (6):

$$\left(\xi_1\right)^2 + \left(\xi_2\right)^2 \le 1 \tag{6}$$

Later, the feasible region of the four in-plane LPs was derived by [32] as (7):

$$\begin{aligned} 2\left(\xi_1\right)^2\left(1-\xi_3\right) + 2\left(\xi_2\right)^2\left(1+\xi_3\right) + \left(\xi_3\right)^2 + \left(\xi_4\right)^2 - 4\xi_1\xi_2\xi_4 \le 1 \\ \left(\xi_1\right)^2 + \left(\xi_2\right)^2 \le 1 \\ -1 \le \xi_i \le 1,\ i = 1,2,3,4 \end{aligned} \tag{7}$$

D. Lamination Angle Retrieval

Once the optimum set of LPs is defined by the optimization algorithm, it is necessary retrieve the fiber angles that are represented by the parameters. This is done by minimizing the least square problem proposed by [30], Equation (8). MMA is used to obtain the optimal fiber angles.

$$\begin{aligned} f(\theta) = &\left(\xi_1^{opt} - \frac{1}{t}\sum_{\mu=1}^{t}\cos\left(2\theta_\mu\right)\right)^2 + \left(\xi_2^{opt} - \frac{1}{t}\sum_{\mu=1}^{t}\sin\left(2\theta_\mu\right)\right)^2 \\ &+ \left(\xi_3^{opt} - \frac{1}{t}\sum_{\mu=1}^{t}\cos\left(4\theta_\mu\right)\right)^2 + \left(\xi_4^{opt} - \frac{1}{t}\sum_{\mu=1}^{t}\sin\left(4\theta_\mu\right)\right)^2 \end{aligned} \tag{8}$$

where $f(\theta)$ is the least square function to be minimized ξ_i^{opt} , $i = 1,2,3,4$ is the optimum LPs, θ_μ ($\mu = 1,2,...,t$) are the design variables, and t is the number of independent fiber angles.

E. Simultaneous TO and Stacking Sequence Optimizaiton

The proposed algorithm overview for solving simultaneously the TO and stacking sequence optimization of composite plates is shown in Figure II.

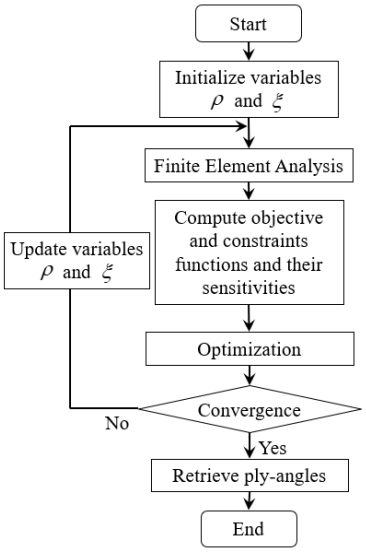

FIGURE II – OVERVIEW OF THE TOPOLOGY AND COMPOSITE STACKING SEQUENCE OPTIMIZATION ALGORITHM STRUCTURE.

The algorithm starts by initializing the TO artificial densities ρ and the set of initial LPs ξ followed by the finite element analysis (FEA). Objective and constraints functions and their respective sensitivities are computed prior to the optimization. Then, the optimization is performed by the Method of Moving Asymptotes (MMA) [33] and convergence is checked. If the problem has not converged the TO and design variables and LPs are updated and the algorithm starts a new iteration with FEA. The optimization terminates when the objective response difference between successive iterations is sufficiently small. After convergence, the lamination angles are retrieved.

The problem is defined as a compliance minimization subject to volume fraction constraint. The simultaneous TO and stacking sequence optimization problem statement is presented in (9).

$$\begin{aligned} &min\ \mathrm{C}(\boldsymbol{u},\boldsymbol{\rho}) = \boldsymbol{u}(\boldsymbol{\rho})^T\,\boldsymbol{k}(\rho)\boldsymbol{u}(\boldsymbol{\rho}) \\ &s.t.\ \ \frac{V(\rho)}{V_i} \le \bar{V} \\ &\qquad 2\left(\xi_1\right)^2\left(1-\xi_3\right) + 2\left(\xi_2\right)^2\left(1+\xi_3\right) + \left(\xi_3\right)^2 + \left(\xi_4\right)^2 - 4\xi_1\xi_2\xi_4 \le 1 \\ &\qquad \left(\xi_1\right)^2 + \left(\xi_2\right)^2 \le 1 \\ &\qquad \forall\rho,\ \rho_i \in (0,1],\ \ i = 1,2,....,m \\ &\qquad \xi_j \in [-1,1],\ \ j = 1,2,3,4 \end{aligned} \tag{9}$$

Identify applicable sponsor/s here. *(sponsors)*

F. Sensitivity Analysis

The MMA optimizer requires the objective and constraint function first order derivative. Thus, deriving (3) with respect to the LPs yields (10):

$$\frac{\partial[A]}{\partial\xi_1}=T\begin{bmatrix}U_{\Delta C} & 0 & 0\\ sym & -U_{\Delta C} & 0\\ sym & sym & 0\end{bmatrix}\quad \frac{\partial[A]}{\partial\xi_2}=T\begin{bmatrix}0 & 0 & U_{\Delta C}/2\\ sym & 0 & U_{\Delta C}/2\\ sym & sym & 0\end{bmatrix}$$
$$\frac{\partial[A]}{\partial\xi_3}=T\begin{bmatrix}U_{\upsilon C} & -U_{\upsilon C} & 0\\ sym & U_{\upsilon C} & 0\\ sym & sym & -U_{\upsilon C}\end{bmatrix}\quad \frac{\partial[A]}{\partial\xi_4}=T\begin{bmatrix}0 & 0 & U_{\upsilon C}\\ sym & 0 & -U_{\upsilon C}\\ sym & sym & 0\end{bmatrix} \tag{10}$$

The compliance C can be defined as (11):

$$C=\boldsymbol{u}_e^T\boldsymbol{k}_e\boldsymbol{u}_e \tag{11}$$

And the elemental stiffness can be defined as (12):

$$\boldsymbol{k}_e=\int_V \boldsymbol{B}^T\boldsymbol{A}\boldsymbol{B}dV \tag{12}$$

where $\boldsymbol{B}$ is the strain-displacement matrix and $\boldsymbol{A}$ is the extensional material stiffness matrix (3). Thus, the compliance sensitivity with respect to the LPs can be defined as (13):

$$\frac{\partial C}{\partial\xi_j}=-\sum_{i=1}^{m}\boldsymbol{u}_i^T\left(\int_V \boldsymbol{B}^T\frac{\partial A}{\partial\xi_j}\boldsymbol{B}dV\right)\boldsymbol{u}_i \tag{13}$$

where m is the number of designable elements. The compliance sensitivities with respect to the artificial design variables is defined as (14):

$$\frac{\partial C}{\partial\rho}=-\sum_{i=1}^{m}\frac{p}{\rho_i}C_i \tag{14}$$

where p is the interpolation penalty factor

The volume fraction V_f constraint sensitivity with respect to the artificial density is defined as (15):

$$\frac{\partial V_f}{\partial\rho}=\frac{V_i}{\sum_{i=1}^{m}V_i} \tag{15}$$

And the two feasible constraints sensitivities are defined as (16):

$$\begin{aligned}
\frac{\partial Feasible_1}{\partial\xi_1}&=4\xi_1(1-\xi_3)-4\xi_2\xi_4\\
\frac{\partial Feasible_1}{\partial\xi_2}&=4\xi_2(1+\xi_3)-4\xi_1\xi_4\\
\frac{\partial Feasible_1}{\partial\xi_3}&=-2\xi_1+2\xi_2+2\xi_3\\
\frac{\partial Feasible_1}{\partial\xi_4}&=2\xi_4-4\xi_1\xi_2\\
\frac{\partial Feasible_2}{\partial\xi_i}&=2\xi_1\quad i=1,2
\end{aligned} \tag{16}$$

III. Numerical Examples

In this article, two examples will be used to test the proposed TO and stacking sequence algorithm. The Messerschmitt-Bölkow-Blohm (MBB) beam and the L-bracket, will demonstrate the capability of the algorithm to simultaneously place the materials over the design space as well as define the optimum ply sequence orientation of the composite plate. In this work, the unidirectional Hexcel 8552 AS4 [34] material will be used for all subsequent problems, and material properties are summarized in Table I. Both MBB and L-bracket examples are solved considering a plate thickness of 2.0 mm or a 10 layers laminate.

TABLE I. – Hexcel 8552 AS4 material properties [34]

	Hexcel 8552 AS4
$E_1=E_2$ $[GPa]$	61.60
$G_{12}=G_{31}$ $[GPa]$	5.72
G_{23} $[GPa]$	4.00
υ_{12}	0.043
γ $\left[\times10^3\,kg/m^3\right]$	1.57
ply thickness [mm]	0.2

A. MBB Beam

The first model is the MBB beam with 1,000 mm × 200 mm × 2 mm. This geometry is meshed using a 5-mm four-node quadrilateral elements yielding 8,000 elements. A diagram of the design space, boundary conditions as well as the symmetry plane definition is shown in Figure III. This problem is solved for a volume fraction constraint of 30% ($\bar{V}\le 0.30$).

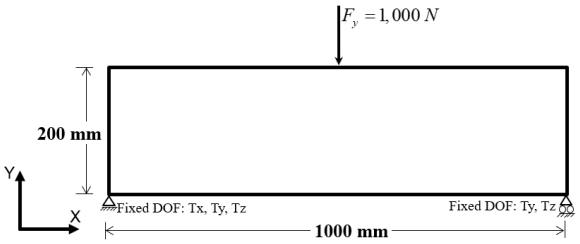

Figure III – Messerschmitt-Bölkow-Blohm beam boundary condition and design space geometry

Figure IV depicts the MBB beam convergency history. The dark solid line indicates a smooth objective function convergence throughout the iterative optimization process. The optimum solution is achieved after 56 iterations. LPs convergence, on the other hand, oscillate mostly during the initial iterations. This behavior is expected as the optimizer is concurrently optimizing the optimum composite lay-up and the material distribution over the design space. After iteration 10, the LPs convergence behavior becomes smoother with the odd LPs, ξ_1 and ξ_3, converging to value of 0.5 and 0.3, respectively. The even LP ξ_2 present the highest oscillation among the four LPs, however, such behavior should not impact

the final results as the even LPs indices tend to be the less important [35].

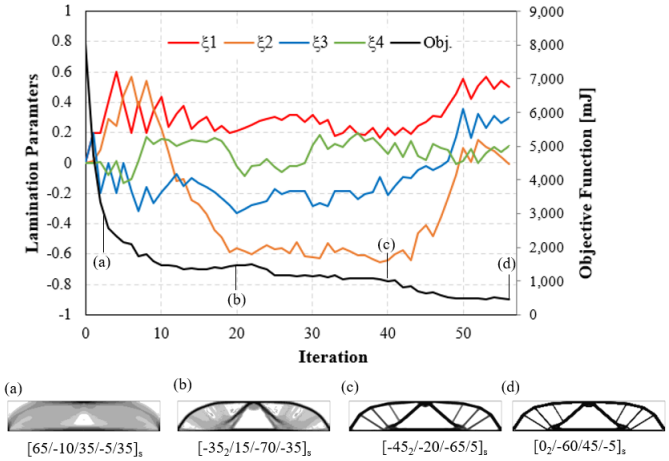

FIGURE IV – MBB BEAM OBJECTIVE AND LAMINATION PARAMTERS CONVERGENCE HISTORY

The stacking sequence for the 10-layers plate is presented at the bottom of Figure IV along with the material distribution over the design domain for selected iterations. It can be seen that the material placement is continuum with the algorithm discretizing the optimum material distribution at each iteration. Angle plies are retrieved with an angular resolution of 5º.

As can be observed in Figure IV, the solver resulted in cross-members with thin members that can be difficult or even infeasible from the point of view of manufacturing. Nevertheless, it is worth mentioning that the components manufacturing process has not been considered in the present studies.

B. L-Bracket

The second problem will be the L-Bracket problem. The geometry presented in Figure V is meshed with 6,500 four-node quadrilateral elements with an average mesh size of 4.0 mm. The plate elements are defined with a constant thickness of 2 mm and a load of 8,000 N. Again, a volume fraction of 30% ($\bar{V} \leq 0.30$) is used as TO constraint.

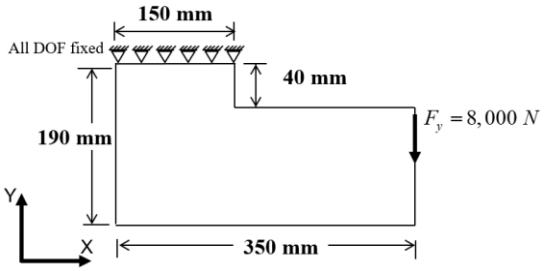

FIGURE V – L-BRACKET BOUNDARY CONDITION AND DESIGN SPACE GEOMETRY

Figure VI shows the L-bracket convergency history. It can be seen that the objective function converges smoothly throughout the optimization. Again, LPs, present oscillation behavior at the initial iterations due to the simultaneous optimization of the material distribution and material stiffness. After few iteration, the LPs start to present a smooth converge behavior. The optimum solution is achieved after 62 iterations.

The 10-layers composite laminate lay-up is shown at the bottom of Figure VI for selected iterations. Again, it can be noticed that the algorithm discretizes the optimum material distribution continuously throughout the optimization. The optimum lay-up is retrieved with an angular resolution of 5º.

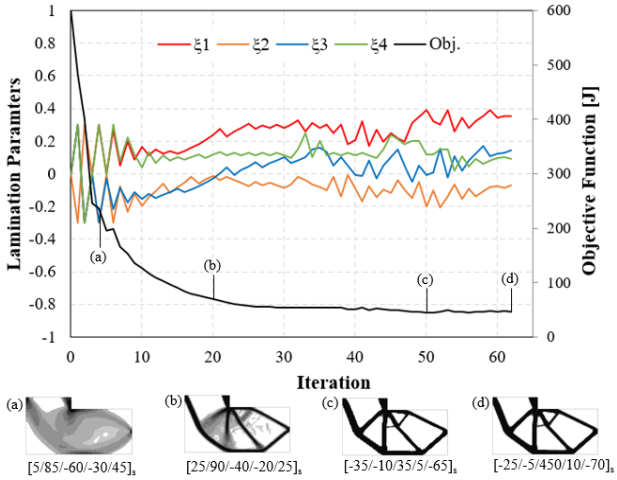

FIGURE VI – L-BRACKET OBJECTIVE AND LAMINATION PARAMTERS CONVERGENCE HISTORY

CONCLUSIONS

This article presented a simultaneous composite plate stacking sequence and topology optimization method for defining the optimum material distribution and laminate lay-up that can help in the additive manufacturing of 3D printed composite plates.

The proposed algorithm extends the application of the traditional topology optimization framework to account for the change in the material stiffness via the stacking sequence of the composite plate. Material stiffness is defined through lamination parameters that presents a convex optimization function with respect to the composite stiffness. An optimum set of lamination parameters are defined as the optimum solution and then the lamination angles are retrieved by means of a minimization function.

Two problem examples are proposed to show the applicability of the proposed algorithm. Both results showed a smooth objective function convergence with lamination parameters oscillating at the initial iterations.

ACKNOWLEDGMENT

This research was funded by the Natural Sciences and Engineering Research Council of Canada (NSERC) and General Motors of Canada. Technical advice and direction were gratefully received from Joe Moore, Ralph Brown, Dan Mepham, Derrick Chow, and Chandan Mozumder at General Motors.

References

[1] Cohen D et al. 3-D printing takes shape McKinsey Quarterly: McKinsey; 2014 [Available from: https://www.mckinsey.com/business-functions/operations/our-insights/3-d-printing-takes-shape#.

[2] Petry C. An additive manufacturing technology undergoes tests and trials on numerous applications as it prepares for takeoff. Modern Metals. 2018 August 2018:3-6.

[3] Airbus. First titanium 3D-printed part installed into serial production aircraft: Airbus; 2017 [Available from: https://www.airbus.com/newsroom/press-releases/en/2017/09/first-titanium-3d-printed-part-installed-into-serial-production-.html.

[4] Sher D. First Chinese Built C919 Commercial Aircraft Flies with Non-Critical 3D Printed Parts 2017 [Available from: https://www.3dprintingmedia.network/first-chinese-built-c919-commercial-aircraft-flies-several-non-flight-critical-3d-printed-parts/.

[5] Blok LG et al. An investigation into 3D printing of fibre reinforced thermoplastic composites. Additive Manufacturing. 2018;22:176-86.

[6] Markforged. Markforged 2020 [Available from: https://markforged.com/.

[7] Composites C. Continuous Composites 2020 [Available from: https://www.continuouscomposites.com/.

[8] Zindani Dand Kumar K. An insight into additive manufacturing of fiber reinforced polymer composite. International Journal of Lightweight Materials and Manufacture. 2019;2(4):267-78.

[9] Kashanian K et al. Motorcycle Chassis Design Utilizing Multi-Material Topology Optimization. SAE Technical Paper Series2020.

[10] Roper S et al. Practical applications for multi-material design utilizing size and topology optimization. 26th CANCAM; May 29 - June 1, 2017; Victoria, British Columbia, Canada2017.

[11] Shah V et al. Multi-Material Topology Optimization Considering Manufacturing Constraints. SAE Technical Paper Series2020.

[12] Vierhout G et al. Multi-Material Topology Optimization as a Concept Generation and Design Tool. SAE Technical Paper Series2019.

[13] Li C et al. Conceptual and detailed design of an automotive engine cradle by using topology, shape, and size optimization. Structural and Multidisciplinary Optimization. 2014;51(2):547-64.

[14] Warwick BT et al. Topology optimization of a pre-stiffened aircraft bulkhead. Structural and Multidisciplinary Optimization. 2019;60(4):1667-85.

[15] Ryan Land Kim IY. A multiobjective topology optimization approach for cost and time minimization in additive manufacturing. International Journal for Numerical Methods in Engineering. 2019;118(7):371-94.

[16] Sabiston Gand Kim IY. 3D topology optimization for cost and time minimization in additive manufacturing. Structural and Multidisciplinary Optimization. 2019;61(2):731-48.

[17] Olsen Jand Kim IY. Design for additive manufacturing: 3D simultaneous topology and build orientation optimization. Structural and Multidisciplinary Optimization. 2020;62(4):1989-2009.

[18] Fritz Kand Kim IY. Simultaneous topology and build orientation optimization for minimization of additive manufacturing cost and time. International Journal for Numerical Methods in Engineering. 2020;121(15):3442-81.

[19] Bendsøe MPand Kikuchi N. Generating optimal topologies in structural design using a homogenization method. Computer Methods in Applied Mechanics and Engineering. 1988;71:197-224.

[20] Bendsoe MP. Optimal shape design as a material distribution problem. Structural Optimization. 1989;1:193-202.

[21] Rozvany GIN et al. Generalized shape optimization without homogenization. Structural Optimization. 1992(4):250-2.

[22] Schmit LAand Farshi B. Optimum laminate design for strength and stiffness. International Journal for Numerical Methods in Engineering. 1973;7:519-36.

[23] Kim CW et al. Stacking sequence optimization of laminated plates. Composite Structures. 1997;39:283-8.

[24] Foldager J et al. A general approach forcing convexity of ply angle optimization in composite laminates. Structural Optimization. 1998;16:201-11.

[25] Khedmati MR et al. Stacking Sequence Optimisation of Composite Panels Subjected to Slamming Impact Loads using a Genetic Algorithm. Latin American Joournal of Solids and Structures. 2013;10:1043-60.

[26] Ferreira RTL et al. Structural Optimization of a Composite Plate subjected to a Small Mass Impact. 2nd International Conference on Engineering Optimization; Lisbon, Portugal2010.

[27] Durand LP. Composite materials research progress. New York: Nova Science Publisher, Inc.; 2008.

[28] Setoodeh S et al. Combined topology and fiber path design of composite layers using cellular automata. Structural and Multidisciplinary Optimization. 2005;30(6):413-21.

[29] Peeters D et al. Combining topology and lamination parameter optimisation. Structural and Multidisciplinary Optimization. 2015;52(1):105-20.

[30] Tong X et al. Optimal Fiber Orientations and Topology of Compliant Mechanisms Using Lamination Parameters. International Conference on Advanced Mechatronic Systems; Beijing, China2015. p. 370-4.

[31] Miki M. Design of Laminated Fibrous Connposite Plates with Required Flexural Stiffness. Recent Advances in Composites in the United States and Japan, ASTM STP 864 J R Vinson and M Taya, Eds, American Society for Testing and Materials, Philadelphia. 1985:387-400.

[32] Hammer VB et al. Parametrization in laminate design for optimal compliance. Inl J Solids Structures. 1997;34(4):415-34.

[33] Svanberg K. The Method of Moving Asymptotes - A new method for structural optimization. International Journal for Numerical Methods in Engineering. 1987;24:359-73.

[34] Marlett K. Hexcel 8552 AS4 Unidirectional Prepreg at 190 gsm & 35% RC Qualification Material Property Data Report. National Institute for Aviation Research; 2011. Contract No.: CAM-RP-2010-002 May 6, 2011 Revision A.

[35] Bohrer RZG et al. Optimization of composite plates subjected to buckling and small mass impact using lamination parameters. Composite Structures. 2015;120:141-52.